POLITECNICO DI TORINO
Repository ISTITUZIONALE

Ultimate Limit State Behavior of RC Members in Bending Strengthened with GFRP Rebars

Original
Ultimate Limit State Behavior of RC Members in Bending Strengthened with GFRP Rebars / Mairone, M., Givonetti, M., Hussain, Z., Gallina, G., Corrado, M., Nanni, A., Masera, D.. - ELETTRONICO. - 770:(2025), pp. 313-329. (3rd International Conference on Resilience, Earthquake Engineering and Structural Health Monitoring (ICONREM) Turin (Italy) June 24-28, 2024) [10.1007/978-3-032-08407-1_26].

Availability:
This version is available at: 11583/3013034 since: 2026-07-13T13:21:21Z

Publisher:
Springer Nature

Published
DOI:10.1007/978-3-032-08407-1_26

Terms of use:

This article is made available under terms and conditions as specified in the corresponding bibliographic description in the repository

Publisher copyright
Springer postprint/Author's Accepted Manuscript

This version of the article has been accepted for publication, after peer review (when applicable) and is subject to Springer Nature's AM terms of use, but is not the Version of Record and does not reflect post-acceptance improvements, or any corrections. The Version of Record is available online at: http://dx.doi.org/10.1007/978-3-032-08407-1_26

(Article begins on next page)

18 November 2026

Ultimate Limit State behavior of RC members in bending strengthened with GFRP rebars

Mattia Mairone[1[0000-0002-3795-7282]], Marco Givonetti[2[0009-0007-5003-6975]], Zahid Hussain[3[0000-0002-5690-9980]], Gianfrancesco Gallina[2[0009-0002-2162-5336]], Mauro Corrado[1[0000-0002-8705-5906]], Antonio Nanni[3[0000-0003-2678-9268]] and Davide Masera [2[0000-0003-2859-9396]].

[1] Politecnico di Torino, 10129 Turin, Italy.
[2] Masera Engineering Group S.r.l., 10121 Turin, Italy.
[3] University of Miami, 33146 Coral Gables, Florida, USA.
mattia.mairone@polito.it

Abstract. In the last decades, composite retrofit technology has been introduced for structural applications in civil engineering. The advantage of reinforcing existing reinforced concrete (RC) members with glass fiber-reinforced polymer (GFRP) bars is to provide the required additional load bearing capacity, while improving maintainability and durability. Being corrosion of steel reinforcement a major cause of damage in ordinary RC structures, the retrofit of existing structures by arranging additional GFRP reinforcing bars externally to the steel ones leads the entire RC section to be less susceptible to subsequent corrosion degradation, thus limiting further repair costs. On the other hand, the use of GFRP rebars reduces the ductility of RC members in bending and, therefore, can be critical specially for structures subjected to seismic excitations. Therefore, a hybrid use of steel and GFRP reinforcement is mandatory, to keep a sufficient level of ductility.

This research aims to highlight the advantages at the Ultimate Limit State (ULS) of the design of repairing/strengthening interventions, such as concrete jacketing, using the innovative retrofitting technique with hybrid steel-GFRP reinforcement. Design models are proposed, based on fundamental theories for RC beams and available literature on failure modes of GFRP reinforced sections. Different solutions are explored by cross-sectional analysis to evaluate the increase in load bearing capacity and the resulting ductility in the bending regime.

Keywords: Glass fiber reinforced polymer (GFRP), Reinforced concrete, Steel-GFRP hybrid reinforced concrete sections, Section analysis, Flexural capacity, Failure mode.

1 Introduction

Corrosion of steel reinforcement in reinforced concrete (RC) structures and infrastructures is a pervasive problem, leading to significant structural degradation and maintenance challenges. When steel bars within concrete corrode, the resulting rust expands and exerts pressure on the surrounding concrete, causing cracks, spalling, and loss of cross-sectional area in both steel and concrete.
This degradation severely compromises the lifespan, structural integrity and load-bearing capacity of the affected elements and escalates the costs associated with their maintenance and repair. In Italy, the issue of corrosion in RC structures is particularly pronounced due to the country's extensive use of such materials in infrastructure and the environmental conditions that accelerate corrosion processes. Coastal areas with high humidity and salt exposure, as well as urban areas with pollution, exacerbate the corrosion of steel reinforcements. Italian infrastructure, which includes a significant number of aging RC bridges, buildings, and marine structures, faces continuous deterioration due to these factors. The introduction of the Multilevel Approach from the Italian Guideline LG20 [1] try to highlight and balance these lacks. This standard evaluates several aspects for safety in the design and verification stages of the engineer at project and verification stage, such as partial safety factors, confidence factors, simplified methods of calculation, limitations on armor and analysis considering linear material behavior. The financial implications of corrosion-related damage in RC structures are substantial. According to a report by the Italian National Research Council, the annual cost of repairing and maintaining RC structures affected by corrosion is estimated to be between €600 million and €1 billion.

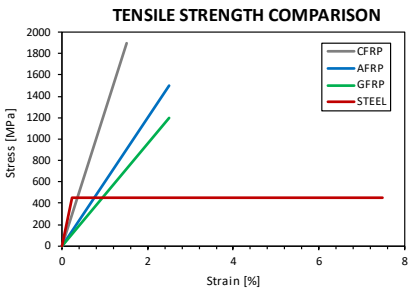


Fig. 1. Constitutive laws for different reinforcing materials.

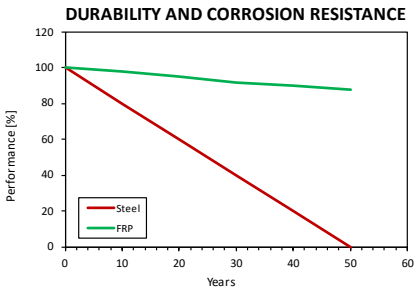


Fig. 2. Durability and corrosion resistance over time.

In an effort to mitigate these challenges, Fiber Reinforced Polymer (FRP) bars have been introduced as a promising alternative to conventional steel reinforcement. Retrofitting steel reinforced concrete (RC) sections with a hybrid solution that incorporates glass fiber-reinforced polymer (GFRP) bars externally to the existing steel bars is an advanced technique aimed at enhancing structural performance and durability. This method involves adding GFRP bars to the concrete section to complement the existing steel reinforcement, thereby improving the overall load-bearing capacity and extending

the lifespan of the structure. GFRP bars exhibit several key mechanical properties that make them suitable for structural reinforcement such as Elastic Modulus typically ranging from 40 GPa to 60 GPa as illustrated in **Fig. 1**; maximum strain for GFRP bars generally around 1.5% to 2.5%; maximum stress in the range of 600 MPa to 1200 MPa [2–5]. The use of GFRP bars in a hybrid reinforcement system offers several advantages, particularly in terms of durability and resistance to corrosion.

The enhanced durability is based on the non-corrosive properties of GFRP bars. This makes GFRP particularly beneficial in harsh environments, such as coastal or industrial areas where exposure to chlorides and other corrosive agents is high. Reduced maintenance costs by preventing corrosion lead to lower lifecycle costs for the structures (**Fig. 2**)[6]. The additional reinforcement provided by GFRP bars increases the load-bearing capacity and overall strength of the RC section.

Despite the benefits, there are some challenges associated with the use of GFRP bars, primarily due to their brittle behavior [7]. Unlike steel, which exhibits ductile behavior and significant plastic deformation before failure, GFRP bars fail in a brittle manner. This lack of ductility can be problematic, particularly in seismic areas where structures must absorb and dissipate energy through plastic deformation. The incorporation of GFRP bars reduces the ductility of the RC section, making it less capable of deforming under load without failure. To mitigate the drawbacks of reduced ductility, it is essential to consider the interaction between steel and GFRP reinforcement in hybrid systems. By combining steel and GFRP bars, the structure can benefit from the strengths of both materials. Steel provides ductility and energy dissipation, while GFRP offers enhanced durability and corrosion resistance. However, the inherent brittleness of FRP bars has restricted their widespread adoption in seismic regions. Structures reinforced with Glass-FRP (GFRP) exhibit brittle failure characteristics without the formation of plastic hinges, which leads to minimal energy dissipation during seismic events. This deficiency in energy dissipation poses a significant barrier to the extensive use of GFRP in seismic zones.

The design of hybrid reinforcement systems should optimize the placement and proportion of steel and GFRP bars to ensure adequate ductility and overall structural performance. This involves detailed analysis and modeling to predict the behavior of the hybrid section under various loading conditions, including seismic events. The concept of hybrid reinforcement, which combines GFRP and steel bars, offers a new strategy to enhance ductility and energy dissipation in GFRP-RC structures. By positioning steel bars on inner side and GFRP on exterior surface of cross-section will provide both energy dissipation as well as corrosion protection and durability.

Therefore, this study is carried out with an intent to understand the possibilities of designing hybrid RC members and provide insights into design philosophies. The aim of this article is providing some methods for consider the material non-linearity during verification of beam cross sections.

A software for sectional verification has been developed and some of its features are illustrated in this article. Software's features include the possibility of defining multiple constitutive laws, since the strength of GFRP is a function of the nominal diameter of the bars.

2 Failure Modes in Hybrid GFRP-Steel RC Sections

The behavior of hybrid sections at Ultimate Limit State (ULS) falls between that of GFRP-RC sections, which manifest only two failure modes (FM) [2,3,8] and that of conventional RC sections with steel bars, which typically exhibit five failure modes [9]: in fact, as evidenced by existing studies [10–14], the integration of GFRP bars reduces the number of failure modes to three:

- FM-I: GFRP reinforcement ruptures after tensile steel reinforcement yielding without concrete crushing (lightly reinforced beam);
- FM-II: concrete crushing occurs after tensile steel reinforcement yielding without rupture of GFRP reinforcement (moderately reinforced beam);
- FM-III: concrete crushing occurs while tensile steel and GFRP reinforcement are in the elastic state (heavily reinforced beam).

These failure modes depend on the geometric percentage of steel ρ_s and GFRP ρ_f present in the section; based on these parameters, it is possible to determine a priori whether the mechanical properties of the reinforcements will be exploited to the maximum or whether the collapse of the section occurs on the concrete side.
Sections characterized by FM-III are unlikely and discouraged, instead, FM-I is quite common in design and application in bridge girders and deck slabs [15].

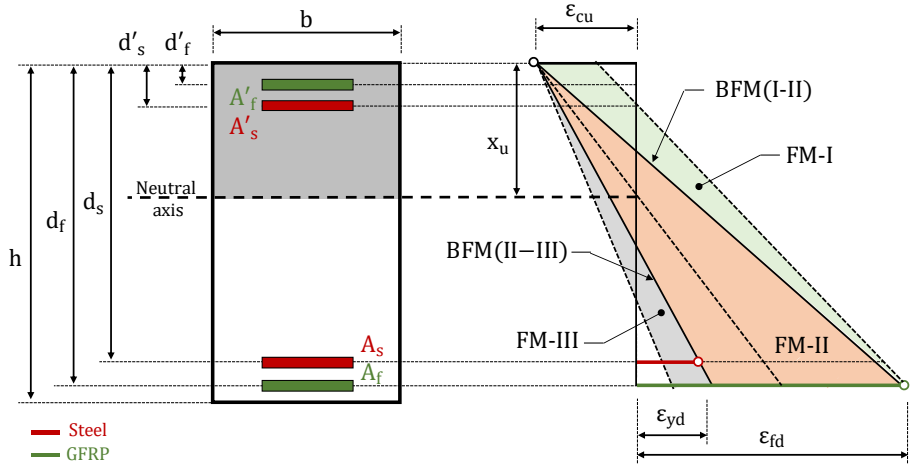


Fig. 3. Strain distribution on a hybrid steel-GFRP RC cross-section at ULS.
(Note: N.A. = neutral axis.)

2.1 Primary Hypotheses for the Analytical Calculation

The current European design codes propose fundamental assumptions for calculating RC sections with both steel and GFRP bars, and either are used for hybrid section design:

- strain varies linearly through the cross-section (sections remain plane);

- equivalent stress block is a valid substitution for nonlinear stress distribution in compressed concrete;
- tensile strength of concrete is ignored;
- perfect bond exists between steel/ GFRP reinforcement and concrete;
- stress-strain response of FRP reinforcement is linear-elastic up to failure;
- steel reinforcement performs the ideal bilinear elastic-plastic behavior;
- compressive strength of GFRP is conservatively neglected.

The cross-section bending capacity is determined by imposing, under conditions of incipient collapse (ULS), that equilibrium to translation and strain compatibility subsist.

2.2 Effect of Reinforcement Ratio on Failure Modes

Based on the geometric ratios of steel ρ_s and GFRP reinforcement ρ_f provided in the section, the ULS resistant configuration must be sought within a specific Failure Mode. In **Table 1** the geometric and mechanical properties of the sections, analysed in the parametric study developed in this paper, are listed.
Hybrid "H" sections are obtained from "RC-S" (reinforced with steel bars) by increasing the sections 10cm per side and adding GFRP reinforcement; "RCS" sections are obtained "H" by replacing the additional reinforcement with steel bars.

Table 1. Sectional input parameters for parametric analysis over A_f and E_f.

	GEOMETRIES		CONCRETE	STEEL'		STEEL		GFRP'			GFRP		
SECTIONS	B	H	f_{cd}	A'_s	f_{yd}	A_s	f_{yd}	A'_f	f'_{fd}	E'_f	A_f	f_{fd}	E_f
	[mm]	[mm]	[MPa]	[mm^2]	[MPa]	[mm^2]	[MPa]	[mm^2]	[MPa]	[GPa]	[mm^2]	[MPa]	[GPa]
RC-S	350	700	17.0	402.1	391.3	1385.4	391.3	-	-	-	-	-	-
H1-E600	550	900	17.0	402.1	391.3	1385.4	391.3	402.1	437.8	60.0	1432.6	430.8	60.0
H2-E600	550	900	17.0	402.1	391.3	1385.4	391.3	402.1	437.8	60.0	5175.4	380.7	60.0
H1a-E448	550	900	17.0	402.1	391.3	1385.4	391.3	402.1	437.8	44.8	1719.1	307.6	44.8
H1b-E448	550	900	17.0	402.1	391.3	1385.4	391.3	402.1	437.8	44.8	5175.4	271.6	44.8
H1-E460	550	900	17.0	402.1	391.3	1385.4	391.3	402.1	437.8	46.0	1885.0	432.0	46.0
H2-E460	550	900	17.0	402.1	391.3	1385.4	391.3	402.1	437.8	46.0	3927.0	432.0	46.0
RCS1-E600	550	900	17.0	402.1	391.3	2818.0	391.3	-	-	-	-	-	-
RCS2-E600	550	900	17.0	402.1	391.3	6560.8	391.3	-	-	-	-	-	-
RCS1a-E448	550	900	17.0	402.1	391.3	3104.6	391.3	-	-	-	-	-	-
RCS1b-E448	550	900	17.0	402.1	391.3	6560.8	391.3	-	-	-	-	-	-
RCS1-E460	550	900	17.0	402.1	391.3	3270.4	391.3	-	-	-	-	-	-
RCS2-E460	550	900	17.0	402.1	391.3	5312.4	391.3	-	-	-	-	-	-

Taking into consideration the hybrid steel-GFRP H1-E600 section, the distribution of reinforcement ratios correlated with the three types of flexural failure modes are schematically illustrated in **Fig. 4**. This domain reflects the balanced deformed configuration of ULS shown in **Fig. 5**, which corresponds to the flexural capacity.

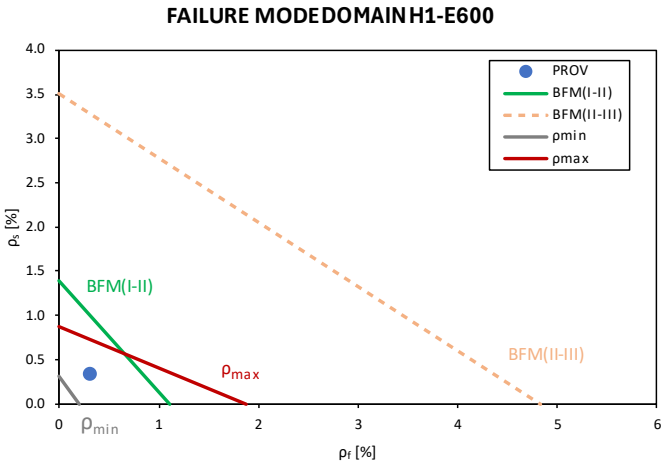


Fig. 4. Failure domain as a function of the reinforcement ratios for the section H1-E600.

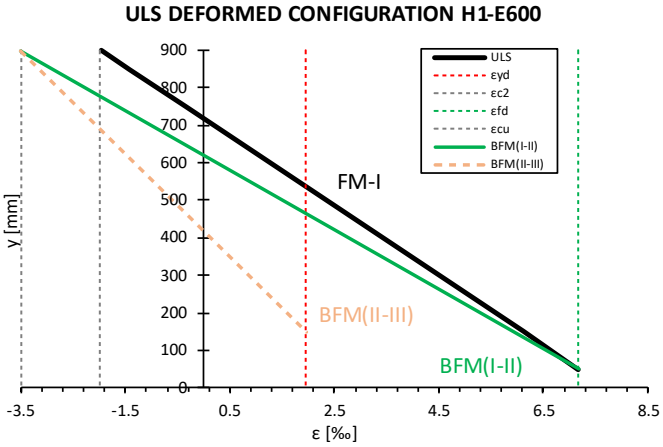


Fig. 5. Deformed configuration FM-I at ULS of H1-E600.

2.2.1 Failure Mode FM-I

GFRP reinforcement rupture is induced at $\varepsilon_f = \varepsilon_{fd}$; yielding of steel reinforcement occurs $\varepsilon_s > \varepsilon_{yd}$ and concrete is not crushed $\varepsilon_c < \varepsilon_{cu}$,
where: ε_{fd} is the ultimate design tensile strain of GFRP, $\varepsilon_{yd} = 1.96‰$ is the yield design strain of steel and $\varepsilon_{cu} = 3.5‰$ is ultimate strain of compressive concrete.

Hybrid RC beam in field FM-I is lightly reinforced with GFRP and steel bars and its ultimate moment is governed by the tensile failure of GFRP reinforcement. As the reinforcement ratio ρ_s and ρ_f increases, the contribution of compressive concrete to flexural capacity and deformation increases.

The balanced failure mode BFM(I-II) is defined as the state with the simultaneous occurrence of concrete crushing and GFRP rupture and $\rho_l^{comp} = \rho_{l,B}^{comp}$ equating **Eq.** (**1**) and **Eq.**(**2**).

$$\rho_l^{comp} = \rho_f + \rho_s\,\eta\,\frac{f_{yd}}{f_{fd}} + \rho'_f\frac{\sigma'_{f(I-II)}}{f_{fd}} + \rho'_s\,\eta\,\frac{\sigma'_{s(I-II)}}{f_{fd}} \tag{1}$$

$$\rho_{l,B}^{comp} = \beta_{1,u}\,\frac{f_{cd}}{f_{fd}} + \frac{\varepsilon_{cu}}{\varepsilon_{cu} + \varepsilon_{fd}} \tag{2}$$

where:

- ρ'_f and ρ'_s:
  geometric percentages of compressed GFRP and steel reinforcement;
- $\sigma'_{f(I-II)}$ and $\sigma'_{s(I-II)}$:
  compression in GFRP bars in the BFM(I-II);
- $\eta = d_s/d_f$:
  ratio of the effective height of tensioned steel to GFRP reinforcement;
- $\beta_{1,u} = 0.85$:
  filling-coefficient of the stress-strain diagram if $\varepsilon_c = \varepsilon_{cu}$ according to EC2;
- f_{cd}, f_{fd} and f_{yd}:
  design stresses of the materials.

For a hybrid RC beam with FM-I, its mechanical reinforcing index ρ_l^{comp} should satisfy the condition of $\rho_l^{comp} < \rho_{l,B}^{comp}$. Furthermore, ρ_l^{comp}should be not less than the minimum GFRP reinforcement ratio $\rho_{f,min}$.

2.2.2 Failure Mode FM-II

GFRP reinforcement is in the elastic state $\varepsilon_f < \varepsilon_{fd}$; the steel reinforcement is yielded $\varepsilon_s > \varepsilon_{yd}$; and concrete is crushed $\varepsilon_c = \varepsilon_{cu}$.
The flexural failure is initiated with steel yielding and then followed by concrete crushing, which is the governing factor.
The balanced failure mode BFM(II-III) is defined as the state with the simultaneous occurrence of concrete crushing and steel yielding and $\rho_{\varepsilon y}^{comp} = \rho_{\varepsilon y,B}^{comp}$ equating **Eq.** (**3**) and **Eq.**(**4**).

$$\rho_{\varepsilon y}^{comp} = \rho_f\,\frac{\alpha'_f\,E'_f\left(\frac{1+\mu}{\eta'} - 1\right) + E_f\left(\frac{1+\mu}{\eta} - 1\right)}{E_s\,\mu\,\eta} + \rho_s\left(1 + \alpha'_s\frac{\varepsilon'_{s(II-III)}}{\varepsilon_{yd}}\right) \tag{3}$$

$$\rho_{\varepsilon y,B}^{comp} = \frac{\beta_{1,u}}{1+\mu}\,\frac{f_{cd}}{f_{yd}} \tag{4}$$

where:

- $\alpha'_f = \rho'_f/\rho_f$ and $\alpha'_s = \rho'_s/\rho_s$:
  geometric percentages of compressed over tensile reinforcements;
- E'_f, E_f and E_s:
  elastic modulus of reinforcements;
- $\eta' = d'_s/d'_f$:
  ratio of the distance of reinforcements from the most compressed fiber of the cross-section;
- $\mu = \varepsilon_{yd}/\varepsilon_{cu}$;
  ratio between the design yield strain of steel and the ultimate strain of concrete;
- $\varepsilon'_{s(II-III)}$: deformation of compressed steel bars in the BFM (II-III).

For hybrid RC beam with FM-II, its mechanical reinforcing index ρ_l^{comp} and $\rho_{\varepsilon y}^{comp}$ should satisfy the condition of $\rho_l^{comp} > \rho_{l,B}^{comp}$ and $\rho_{\varepsilon y}^{comp} < \rho_{\varepsilon y,B}^{comp}$.

2.2.3 Failure Mode FM-III

This section is so heavily armored (the amount of bars required to be in this range is not permissible compared with the geometric dimensions of the section), it has non-ductile behavior, and the materials cannot fully exploited their strength properties.
In this failure mode, both GFRP and steel reinforcement are in the elastic state: $\varepsilon_f < \varepsilon_{fd}$ and $\varepsilon_s < \varepsilon_{yd}$; while concrete is crushed at $\varepsilon_c = \varepsilon_{cu}$.
Its effective reinforcement stiffness $\rho_{\varepsilon y}^{comp}$ must satisfy the condition $\rho_{\varepsilon y}^{comp} > \rho_{\varepsilon y,B}^{comp}$.

2.3 Design Codes Requirements

In practical design, it is recommended to use “ductile sections” at least bringing the steel to yield when the incipient collapse condition occurs. Among the three failure modes, it is preferable for the section behavior to be FM-II as it is more progressive and has higher ductility or deformability than the others and the strength properties of materials, such as GFRP, steel, and concrete, can be fully exploited.
However, the sizing of hybrid sections must simultaneously meet the limitations imposed by EC2 and NTC18 [16,17] on steel reinforcement:

- limitations on ρ_s and ρ'_s and the height of the compressed zone at the ULS to ensure sufficient ductility to the section;
- adequate bar spacing to satisfy the Service Limit State of (SLS);

and the ones imposed by CNR-DT 203/2006, fib Bulletin 40 and ACI CODE-440.11-22 [2,3,8] for GFRP bars that relate more to construction details.
Hussain and Nanni [18,19] have highlighted the fact that the required anchorage lengths for GFRP-RC members pose implementation challenges. A hybrid section with both

steel and GFRP reinforcement would require comparatively lesser values, hence avoiding detailing challenge for GFRP-RC members.

3 Ductility Evaluation

Ductility of conventional steel RC members is defined as the ratio of deformations (curvature, displacement) at the ultimate state to that at steel yielding state. The traditional ductility indices are not applicable to GFRP-RC members since the members do not show the yielding behavior: European standards [20,21] defines ductility for conventional RC sections, so the ductility for hybrid sections can be derived

$$\mu_{\mathrm{RC-steeel}} = \frac{\chi_{\mathrm{ultimate}}}{\chi_{\mathrm{yielding}}} \;\; ; \;\; \mu_{\mathrm{RC-hybrid}} = \frac{\chi_{\mathrm{rupture}}}{\chi_{\mathrm{yielding}}} \tag{5}$$

The findings available in literature indicate that Hybrid RC sections can achieve the desired ductility by carefully balancing the ratio of GFRP to steel reinforcement. To accurately assess the ductility of RC hybrid members, Pang et al. [22] proposed a ductility index that considers two factors of deformability and energy absorption capacity.

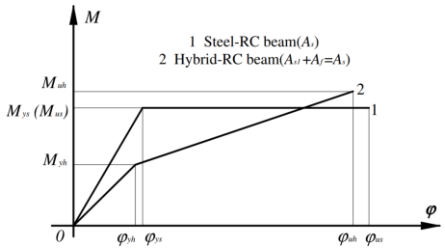


Fig. 6. Ideal moment-curvature relations for RC beams having the same area of reinforcement [22].

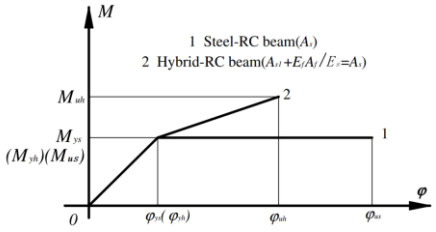


Fig. 7. Ideal moment-curvature relations for RC beams having the same axial stiffness of reinforcement [22].

When the sum of the area of steel reinforcement A_s and the area of GFRP reinforcement A_f in a hybrid-RC beam is equal to the area of steel reinforcement A_s^* in a steel-RC beam, i.e., $A_s + A_f = A_s^*$, the behavior shown in the **Fig. 6** occurs.

By considering the different elastic moduli of the steel and GFRP bars, the effective reinforcement stiffness converts GFRP reinforcements into equivalent steel reinforcements. In this way, meaningful comparisons among steel-RC beams, GFRP -RC beams, and hybrid-RC beams are possible.

When the sum of the steel reinforcement area A_s and the GFRP reinforcement effective area $A_f(E_f/E_s)$ in a hybrid-RC beam is equal to the steel reinforcement area A_s^* in a steel-RC beam, namely, $A_s + A_f(E_f/E_s) = A_s^*$, the moment-curvature relationships of the RC beams are presented in **Fig. 7**.

In this study, the ductility index proposed by Pang et al. [22,23] and Binbin et al. [22,23] is adopted, which offers a comprehensive assessment of deformability and energy dissipation capacity. This index was applied based on the mechanical properties and combination of GFRP and steel reinforcement, providing a robust framework for evaluating the structural performance of hybrid sections.

$$\mu_h = \psi \frac{D_{u,h}}{D_{y,h}} \tag{6}$$

$$\psi = U_H / U_S \leq 1.0 \tag{7}$$

where: ψ is the ductility reduction factor; $D_{u,h}$ is the ultimate deformation (i.e., curvature, rotation and displacement) of the hybrid-RC beam; $D_{y,h}$ is the deformation of the hybrid-RC beam at the commencement of steel yielding; U_H is the area under the moment-curvature diagram of the hybrid-RC beam and U_S is the area under the moment-curvature diagram of the steel-RC beam with the equivalent steel area being equal to $A_s + A_f(E_f/E_s)$.

Note that **Eq.(8)** is in the generic form but must be detailed according to whether the section is in FM-I, FM-II or FM-III.

$$U_H = \frac{M_{y,h}\,\varphi_{y,h}}{2} + \frac{\left(M_{y,h} + M_{u,h}\right)\left(\varphi_{u,h} - \varphi_{y,h}\right)}{2} \tag{8}$$

$$U_S = \frac{M_{y,s}\,\varphi_{y,s}}{2} + \frac{\left(M_{y,s} + M_{u,s}\right)\left(\varphi_{u,s} - \varphi_{y,s}\right)}{2} \tag{9}$$

where: $M_{y,h}$ and $M_{y,s}$are the yield moments of hybrid RC beam and steel RC beam, respectively; and $\varphi_{y,h}$ and $\varphi_{y,s}$ are the corresponding yield curvatures, respectively.

4 Development of Software

4.1 Bases and Assumptions of the Fiber-Code

This code has the feature of solving fiber cross sections. The fiber method, as shown in **Fig. 8**, involves dividing a section into several sub-elements called "fibers," which have certain mechanical properties derived from the constitutive law considered.

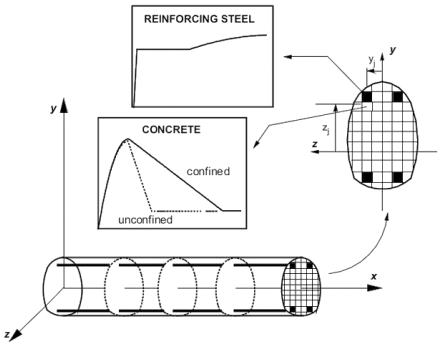


Fig. 8. Fiber discretization [24].

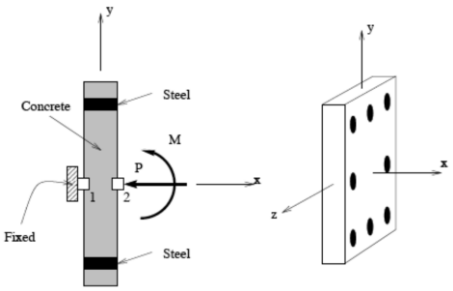


Fig. 9. *Zero-length section* for fiber section analysis [24].

4.2 Fiber-Code Development

The Fiber-Code was developed with *Python* using *Opensees* (*OpenseesPy* environment [25]), a framework for structural analysis developed at the University of Berkeley. The *Zero-length section* is used to implement the cross-section verification as shown in **Fig. 9**. The main component inherent to section elements, loads and the type of analysis [26] performed were used. For the flexural analysis, a displacement-controlled method was preferred as it allows the behavior of the concrete fibers and bars to be observed even after the critical peak.

To enable this analysis, it was essential to define an integration method [27]. In this instance, since the fiber mesh could be modified, it was crucial to implement an algorithm that would determine the suitable integration method for each specific case through trial and error. Regarding the materials assigned to fibers, in according to standards [16,17], it is possible to refer to libraries previously developed by various researchers and made available on *Opensees*, as illustrated in **Fig. 10**. Specifically, this code utilizes *Concrete01* as the concrete model. For ordinary steel reinforcement the *Steel01* model was used. The GFRP bars were modeled with a uniaxial elastic material named *Elastic*. All materials were limited in terms of deformation according with current European codes [3,17].

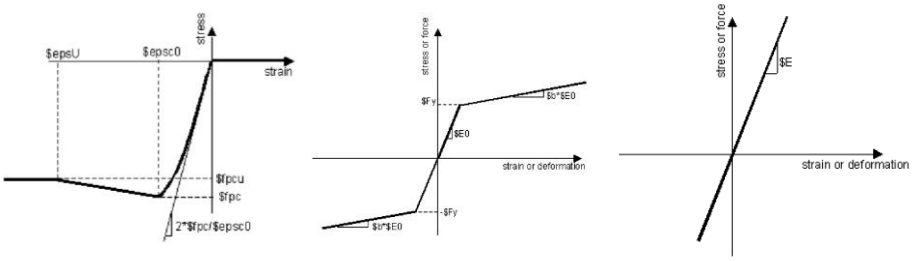


Fig. 10. Stress–strain relationships of *Concrete01*, *Steel01* and *Uniaxial Elastic* [24] (from left to right).

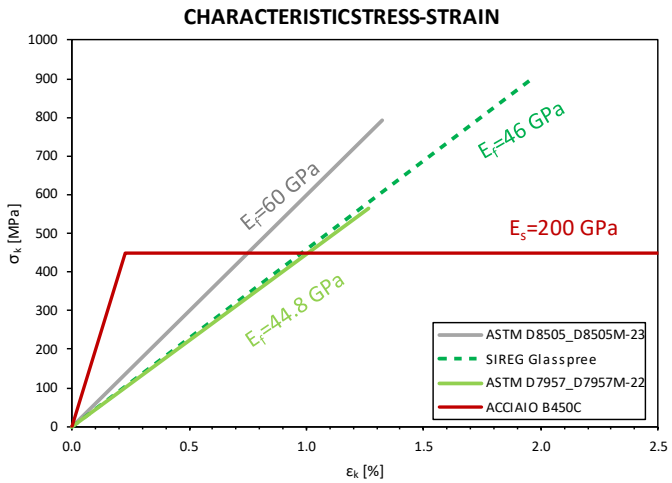


Fig. 11. Stress-strain relationship for GFRP bar diameter 29 mm.

The utility of this code is to obtain the moment-curvature diagram [28] to observe the bending behaviour of the hybrid-RC sections.

4.3 Fiber-Code Validation

The validation of the Fiber-Code is achieved by analytical calculation [29,30]. The same materials with the same stress and strain values are used for ULS.
In particular, referring to **Fig. 10**, the following constitutive laws have been used: a parabola-rectangle for concrete, a bilinear with perfect plasticity for steel, and a simple linear-elastic up to failure for GFRP.

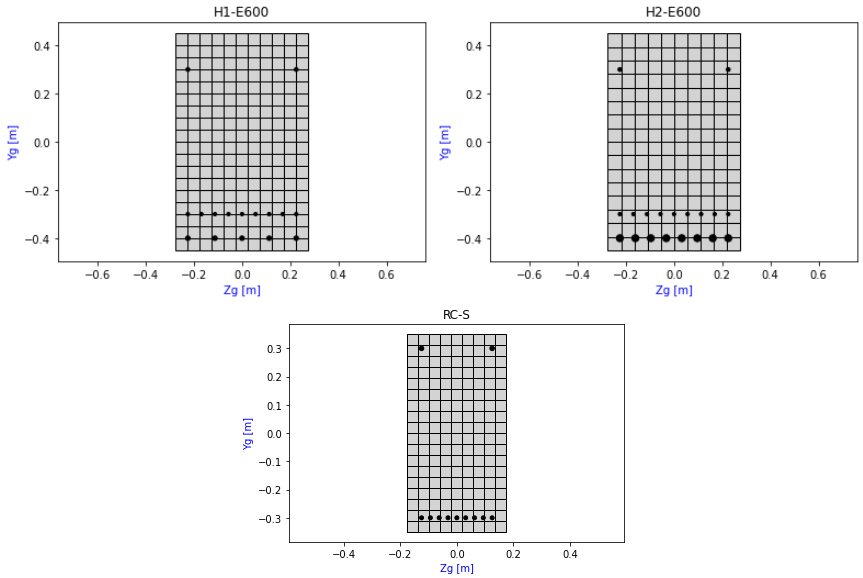


Fig. 12. Validated Fiber-Sections (RC-S, H1-E600, H2-E600).

The contribution of GFRP bar strength is present in the general analytical formulations but is cautiously neglected if the bars are compressed.
The validation is carried out by analysing three sections, namely RC-S, H1-E600 and H2-E600, presenting the geometric and reinforcement data shown in **Table 1**. The results, in terms of resistant bending moment given by the code and the validation calculations, are shown in **Fig. 13**.

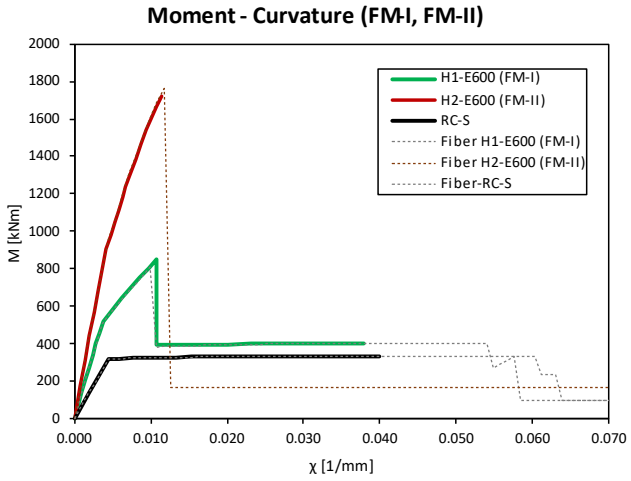


Fig. 13. Numerical and analytical moment-curvature diagrams of RC-S, H1-E600, H2-E600.

It is noted that the resistant moment value provided by the Fiber-Code is in good agreement with the results obtained with the analytical calculations. The ultimate curvature values obtained from analytical calculation is the same of the code. Following the results obtained and the considerations made it is possible to consider the code as validated.

5 Parametric study

A repair/strengthening intervention of an existing RC section by concrete jacketing with additional GFRP bars is simulated and the twofold aspect of strength and ductility is evaluated.
The implemented parametric analyses considered:

- GFRP bars with different mechanical properties (bars with an elastic modulus of $E_f = 44.8$ GPa and high-strength with $E_f = 46$ GPa [5] and $E_f = 60$ GPa [4]) as shown in **Fig. 11**;
- different reasonable value of additional GFRP tensioned reinforcement ρ_f to explore different failure modes (FM-I and FM-II) consistent with the limitations that are imposed by current European and American design codes;
- the hybrid sections were reinforced with GFRP bars of different diameters:
    - 16mm diameter for all sections (compressed reinforcement);
    - 19 mm diameter for sections H1a-E448, H1-E460 and H1-E600;
    - 25 mm diameter for sections H2-E460;
    - 29 mm diameter for sections H1b-E448 and H2-E600.

The aim is to capture the transition between allowable failure modes [31] and the change in ductility and bending capacity produced by the introduction of GFRP bars.
With reference to **Fig. 4**. changing the additional GFRP reinforcement means moving horizontally by varying ρ_f and keeping ρ_s of the original "RC-S" pre-intervention section constant choosing combinations of (ρ_f-ρ_s) that satisfy the design codes requirements highlighted by ρ_{max} line. In particular, the sections "RCS" was also studied by simulating the insertion of additional steel reinforcement equal to the additional GFRP bars in the "H" sections.

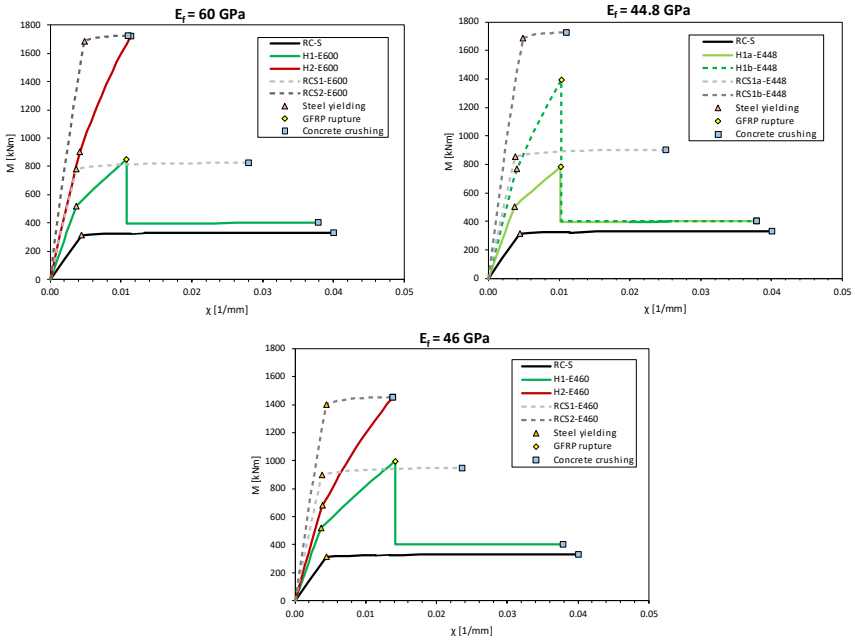


Fig. 14. Moment-curvature diagrams of parametric analysis.

Instead, **Table 2** (where 1 is related to same area and 2 same axial stiffness of reinforcement) shows the limiting values of the mechanical percentages of steel reinforcement and GFRP separating Failure Modes. Along with the type of failure for which the cross-sections were calculated, the calculation of ductility in bending is also shown.

Table 2. Parametric Failure Modes and ductility.

SECTIONS	ρ_l^{comp}	$\rho_{l,B}^{comp}$	ρ_{esy}^{comp}	$\rho_{esy,B}^{comp}$	Failure Mode	M_{Rd}	$\chi_{u(f)}/\chi_y$	ψ_1	ψ_2	μ_{h1}	μ_{h2}
	[%]	[%]	[%]	[%]		[kNm]	Eq. (5)	Eq. (7)		Eq. (6)	
RC-S	-	-	-	-	-	331.0	9.02	-	-	-	-
H1-E600	0.51	1.05	0.36	2.26	FM-I	849.6	2.92	0.33	0.34	2.13	3.22
H2-E600	1.33	1.29	0.73	2.26	FM-II	1724.1	2.74	0.75	0.62	1.77	4.03
H1a-E448	0.65	1.51	0.34	2.26	FM-I	784.0	2.78	0.29	0.30	1.71	2.92
H1b-E448	1.42	1.85	0.60	2.26	FM-I	1393.9	2.58	0.55	0.46	1.30	3.41
H1-E460	0.62	0.86	0.36	2.26	FM-I	994.9	3.84	0.50	0.51	2.80	4.95
H2-E460	1.06	0.86	0.52	2.26	FM-II	1453.6	3.55	0.72	0.66	2.27	5.37
RCS1-E600	-	-	-	-	-	825.2	7.61	-	-	-	-
RCS2-E600	-	-	-	-	-	1726.8	2.26	-	-	-	-
RCS1a-E448	-	-	-	-	-	902.5	6.65	-	-	-	-
RCS1b-E448	-	-	-	-	-	1726.8	2.26	-	-	-	-
RCS1-E460	-	-	-	-	-	946.7	6.18	-	-	-	-
RCS2-E460	-	-	-	-	-	1452.3	3.10	-	-	-	-

Conclusions

In this paper, the effects the ratio of GFRP to steel reinforcement, type of GFRP reinforcement, on the flexural performance of the beams, were parametrically investigated simulating the structural reinforcement of concrete jacketing with GFRP bars and compared with the traditional done with steel bars.
From an RC section, the influence of inserting additional GFRP bars was studied, compared with the classical concrete jacketing intervention with steel bars. In addition, compared to the works in the literature, the presence of compressed reinforcement was also considered, which conditions the maximum geometric percentage of steel tensioned reinforcement.
The following main conclusions can be drawn.

- Heavily-reinforced sections (FM-III) are impractical because of the excessive quantity of reinforcement needed, and for this reason it remains a theoretical Failure Mode with no ductility.
- The graph representing (ρ_f-ρ_s) that describes in its generality all the possible domains of the Failure Modes of hybrid steel-GFRP sections represents a useful tool that speeds up the design of these sections and directly allows to check eligibility against the requirements imposed by the current design codes.
- The validation of the Fiber Code written in *OpenseesPy*, consistent with the constitutive laws of materials and their ultimate stresses and strains, allows its use for a variety of geometric shapes and more complex reinforcement arrangements.
- With the same amount of additional steel/GFRP reinforcement:
    - the hybrid sections in FM-II with GFRP bars having elastic modulus $E_f = 46$ GPa and $E_f = 60$ GPa have similar values of bending capacity and ductility, however if in FM-I they are comparable in strength and the steel sections have higher ductility;
    - if the original section is strengthened with GFRP bars having elastic modulus $E_f = 44.8$ GPa, which also have lower strength, compared to sections reinforced with steel bars they are less performing for both strength and ductility.

Acknowledgements

This publication is part of the project PNRR-NGEU which has received funding from the MUR - DM 352/2022.

References

1. Ministero delle Infrastrutture e dei Trasporti, C.S. dei L.P. Linee Guida per La Classificazione e Gestione Del Rischio, La Valutazione Della Sicurezza Ed Il Monitoraggio Dei Ponti Esistenti. **2022**.
2. fib Bulletin 40 *FRP Reinforcement in RC Structures : Technical Report*; International Federation for Structural Concrete, 2007; ISBN 9782883940802.
3. CNR-DT 203/2006 *Istruzioni per La Progettazione, l'Esecuzione Ed Il Controllo Di Strutture Di Calcestruzzo Armato Con Barre Di Materiale Composito Fibrorinforzato*; Roma, 2006;
4. D8505_D8505M-23 Standard Specification for Basalt and Glass Fiber Reinforced Polymer (FRP) Bars for Concrete Reinforcement 1., doi:10.1520/D8505_D8505M-23.
5. D7957_D7957M-22 Standard Specification for Solid Round Glass Fiber Reinforced Polymer Bars for Concrete Reinforcement 1., doi:10.1520/D7957_D7957M-22.
6. Ye, Y.Y.; Zeng, J.J.; Li, P.L. A State-of-the-Art Review of FRP-Confined Steel-Reinforced Concrete (FCSRC) Structural Members. *Polymers (Basel)* 2022, *14*.
7. Nanni, A.; De Luca, A.; Jawaheri Zadeh, H. *Reinforced Concrete with FRP Bars*; CRC Press, 2014; ISBN 9780203874295.
8. ACI Committee 440; American Concrete Institute *Building Code Requirements for Structural Concrete Reinforced with Glass Fiber-Reinforced Polymer (GFRP) Bars: Code and Commentary*; ISBN 9781641951937.
9. Givonetti, M.; Mairone, M.; Asso, R.; De Luca, E.; Grateron, L.A.B.; Masera, D.; Marano, G.C. Non-Linear Analysis of R.C. and P.R.C. Girder Bridges. *Designs (Basel)* **2023**, *7*, doi:10.3390/designs7040102.
10. Ruan, X.; Lu, C.; Xu, K.; Xuan, G.; Ni, M. Flexural Behavior and Serviceability of Concrete Beams Hybrid-Reinforced with GFRP Bars and Steel Bars. *Compos Struct* **2020**, *235*, doi:10.1016/j.compstruct.2019.111772.
11. Yang, Y.; Pan, D.; Wu, G.; Cao, D. A New Design Method of the Equivalent Stress–Strain Relationship for Hybrid (FRP Bar and Steel Bar) Reinforced Concrete Beams. *Compos Struct* **2021**, *270*, doi:10.1016/j.compstruct.2021.114099.
12. Qin, R.; Zhou, A.; Lau, D. Effect of Reinforcement Ratio on the Flexural Performance of Hybrid FRP Reinforced Concrete Beams. *Compos B Eng* **2017**, *108*, 200–209, doi:10.1016/j.compositesb.2016.09.054.
13. Araba, A.M.; Ashour, A.F. Flexural Performance of Hybrid GFRP-Steel Reinforced Concrete Continuous Beams. *Compos B Eng* **2018**, *154*, 321–336, doi:10.1016/j.compositesb.2018.08.077.
14. Peng, F.; Asce, S.M.; Xue, W. Analytical Approach for Flexural Capacity of FRP Prestressed Concrete T-Beams with Non-Prestressed Steel Bars. **2018**, doi:10.1061/(ASCE).

15. Gilbert, R.I.; Smith, S.T. Strain Localization and Its Impact on the Ductility of Reinforced Concrete Slabs Containing Welded Wire Reinforcement. *Advances in Structural Engineering* **2006**, *9*, 117–127, doi:10.1260/136943306776232837.
16. Ministero delle Infrastrutture e dei Trasporti Aggiornamento Delle Norme Tecniche per Le Costruzioni NTC2018. **2018**.
17. European Committee for Standardization *EN 1992-1-1 (2005) Eurocode 2: Design of Concrete Structures*; Brussels, Belgium, 2005;
18. Hussain, Z.; Lin, J.; Trussoni, M.J.; Nanni, A. Thickness of Glass Fiber-Reinforced Polymer-Reinforced Concrete Slabs. *ACI Struct J* **2023**, *120*, 187–196, doi:10.14359/51738506.
19. Hussain, Z.; Nanni, A. Design and Detailing of Glass Fiber-Reinforced Polymer-Reinforced Concrete Beams According to ACI CODE-440.11-22. *ACI Struct J* **2023**, *120*, doi:10.14359/51738744.
20. European Committee for Standardization EN 1998-1-1 (2005) Eurocode 8: Design of Structures for Earthquake Resistance 2005.
21. Circolare 21 Gennaio 2019, n. 7 C.S.LL.PP. Istruzioni per l'applicazione Dell'aggiornamento Delle Norme Tecniche per Le Costruzioni.
22. Pang, L.; Qu, W.; Zhu, P.; Xu, J. Design Propositions for Hybrid FRP-Steel Reinforced Concrete Beams. *Journal of Composites for Construction* **2016**, *20*, doi:10.1061/(asce)cc.1943-5614.0000654.
23. Zhou, B.; Wu, R.Y.; Liu, Y.; Zhang, X.; Yin, S. Flexural Strength Design of Hybrid Frp-steel Reinforced Concrete Beams. *Materials* **2021**, *14*, doi:10.3390/ma14216400.
24. Opensees Homepage Https://Opensees.Berkeley.Edu.
25. OpenseesPy Hompage Https://Openseespydoc.Readthedocs.Io/En/Latest/.
26. Carpinteri, A. *Analisi Non-Lineare Delle Strutture*; Pitagora Editrice: Bologna, 1997;
27. Bontempi, F. Analisi Strutturale Non Lineare: Modellazione, Algoritmi, Aspetti Critici 2020.
28. Givonetti, M.; Mairone, M.; Asso, R.; Bohorquez Grateron, L.A.; Masera, D.; Marano, G.C. Non-Linear Analysis of RC and PRC Structures Towards a Maximum Exploitation of the Plastic Reserves of the Materials. In *Building for the Future: Durable, Sustainable, Resilient*; Ilki, A., Ed.; Springer Nature Switzerland, 2023; pp. 209–218 ISBN 978-3-031-32518-2, doi.org/10.1007/978-3-031-32519-9_19.
29. Cosenza, E.; Manfredi, G.; Pecce, M. *Strutture in Cemento Armato: Basi Della Progettazione*; Terza edizione.; Hoepli, 2019;
30. Nanni, A. *Guide for the Design and Construction of Concrete Reinforced with FRP Bars (ACI 440.1R-03)*; 2005;
31. Corrado, M.; Ventura, G.; Carpinteri, A. Experimental Evidences of Flexural to Shear to Crushing Failure Mode Transition in Reinforced Concrete Beams without Stirrups. *Eng Struct* **2022**, *271*, doi:10.1016/j.engstruct.2022.114848.